IEEE Open Journal of the
Industrial Electronics Society

Received 27 April 2025; revised 8 June 2025; accepted 30 June 2025. Date of publication 3 July 2025;
date of current version 23 July 2025. The review of this article was arranged by Associate Editor D. Vinnikov.

Digital Object Identifier 10.1109/OJIES.2025.3585749

Isomorphism-Based Fast Simulation of Mismatched Photovoltaic Arrays

D. DEL GIUDICE [1] (Member, IEEE), A. DOLARA [2], J. D. BASTIDAS-RODRIGUEZ [3,5], G. SPAGNUOLO [3] (Fellow, IEEE), A. M. BRAMBILLA [1] (Senior Member, IEEE), AND F. BIZZARRI [1,4] (Senior Member, IEEE)

[1]Politecnico di Milano, DEIB, I20156 Milano, Italy
[2]Politecnico di Milano, DENG, I20156 Milano, Italy
[3]Università di Salerno, DIEM, 84084 Fisciano (SA), Italy
[4]Advanced Research Center on Electronic Systems for Information and Communication Technologies E. De Castro (ARCES), University of Bologna, 41026 Bologna, Italy
[5]Universidad Nacional de Colombia, Facultad de Ingeniería y Arquitectura, Manizales (Caldas) 170004, Colombia

CORRESPONDING AUTHOR: F. BIZZARRI (e-mail: federico.bizzarri@polimi.it).

This work was supported in part by the Italian MUR under Grant PRIN 2022 PNRR "An isomorphism-based digital twin for mismatched photovoltaic arrays control and diagnosis", and in part by the European Union – NextGenerationEU CUP under Grant D53D23016010001, Grant P2022EN3AL.

ABSTRACT Mismatched operating conditions occur very frequently in photovoltaic arrays, especially in urban installations or those that are commonly referred to as agrivoltaic. Mismatches are not only due to partial shading, but also to modules' construction tolerances and installation mistakes, to maintenance operations, to a different effect of aging on modules, to an uneven distribution of dust, pollution, and snow on the module surfaces. The simulation of photovoltaic arrays operating in mismatched conditions is required in many applications, from plant design to model-based control, from monitoring and diagnosis up to the implementation of a digital twin. Some applications require not only an extreme granularity level (even at the single cell or fractions of it) but also a very fast computation compatible with real-time applications, running on embedded processors. This article introduces a new approach to the simulation of mismatched photovoltaic arrays based on isomorphism. The approach exploits similarities among subsections of the array to minimize the number of nonlinear equations modeling it. The lower the simulation accuracy required, the smaller the rank of the system of equations to solve. The application examples proposed in the article, concerning a PV array affected by a partial shading by nearby objects that changes during the day and a faulty PV field made up of half-cut modules, allow one to quantify the reduction in model complexity and the consequent computation time granted by the proposed technique as a function of the desired accuracy of the simulation results.

INDEX TERMS Circuit simulation, circuit theory, mismatched operating conditions, numerical methods, photovoltaics (PVs), partial shading, renewable energy sources, time-domain analysis.

NOMENCLATURE

General Acronyms and Symbols

IC	Integrated circuit.
PV	Photovoltaic.
SC	Subcircuit.
STR	String.
STK	Stack.
MD	Module.
SMD	Submodule.
CL	Cell.
STC	Standard test condition.

Physical Constants

q	Electron charge ($1.60217663 \cdot 10^{-19}$ C).
k_B	Boltzmann const. ($1.380649 \cdot 10^{-23}$ $m^2 kg\, s^{-2} K^{-1}$).
Z_c	Equivalent 0°C in Kelvin scale (273.15 [K]).
S_0	Reference solar irradiance at STC (1000 Wm^{-2}).
T_0	Reference cell temperature at STC (298.15 K).

Photovoltaic Array

V_{PV}	PV voltage [V].
I_{PV}	PV current [A].
P_{PV}	PV generated power [W].

Photovoltaic String

V_{STR}	STR voltage [V].
I_{STR}	STR current [A].
M_m	# of MD connected in series.
M_a	# of STR connected in parallel.

Photovoltaic Module

V_{MD}	MD voltage [V].
I_{MD}	MD current [A].
M_s	# of SMDs connected in series.
M_p	# of STKs of SMD connected in parallel.
V_{STK}	Voltage across an STK of SMDs [V].
I_{STK}	Current through an STK of SMDs [A].

Photovoltaic Submodule

V_{SMD}	SMD voltage [V].
I_{SMD}	SMD current [A].
N_s	Number of CL connected in series.
T_{bp}	Bypass diode operating temperature [K].
I_{bp}	Bypass diode current [A].
I_{bps}	Bypass diode saturation current [A].

Photovoltaic Cell

V	CL voltage [V].
I	CL current [A].
I_{ph}	Photo-generated current [A].
S	Solar irradiance [Wm^{-2}].
T_a	Ambient temperature [°C].
T_c	Cell operating temperature [K].
NOCT	Normal operating cell temperature [°C].
R_{sh}	Parasitic resistance modeling junction losses [Ω].
R_s	Parasitic resistance due to interconnects [Ω].
D_c	Junction implementing the cells (CLs).
v_{jn}	CL junction voltage [V].
I_{sc0}	Short-circuit current in STC [A].
I_{s0}	Junction dark saturation current in STC [A].
I_s	Junction saturation current [A].
m	Ideality/quality factor of D_c.
V_{th}	The $\frac{k_B T_c}{q}$ thermal voltage [V].
$\alpha_{I_{\text{sc}}}$	Short-circuit current thermal coefficient [AK^{-1}].

Isomorphic Photovoltaic Array Parameters

Ξ^{ξ}	Isomorphic tag of $\xi \in \{\text{CL, SMD, STK, MD, STR}\}$.
$\mathscr{A}$	# of clusters of isomorphic STR in the PV array.
$\mathscr{V}$	# of isomorphic quantities at CL or SMD level.
M_{a_i}	# of STR in parallel and isomorphic with STR_i.
$\mathscr{M}_i$	# of clusters of MD in STR_i.
$M_{m_{ij}}$	# of MD in series and isomorphic with MD_{ij}.
$\mathscr{P}_{ij}$	# of clusters of STK in MD_{ij}.
$M_{p_{ijk}}$	# of STK in parallel and isomorphic with STK_{ijk}.
$\mathscr{S}_{ijk}$	# of clusters of SMD in STK_{ijk}.
$M_{s_{ijkh}}$	# of SMD in series and isomorphic with SMD_{ijkh}.
$\mathscr{C}_{ijkh}$	# of clusters of CL in SMD_{ijkh}.
$N_{s_{ijkhq}}$	# of CL in series and isomorphic with CL_{ijkhq}.
$\mathscr{Z}_{\text{SMD}}$	# of equations with isomorphism at SMD level.
$\mathscr{Z}_{\text{CL}}$	# of equations with isomorphism at CL level.

I. INTRODUCTION

Photovoltaics (PVs) is one of the main technologies for the world energy transition [1] with 1.6 TW of cumulative capacity and 446 GW installed in 2023 [2]. An increasing number of new plants will be integrated into existing contexts (e.g., in buildings, in urban scenarios, in agriculture). Their design requires PV arrays simulation approaches that are more sophisticated than in the past, when the majority of the PV plants were installed on flat surfaces, with all the modules (MDs) having the same orientation toward the Sun, without any obstacle in the neighborhood. Indeed, building integrated PV arrays and agrivoltaic PV strings (STRs), just to mention two scenarios, require an accurate modeling of the mismatching effects due to partial shading, dust, snow, pollution, nonuniform albedo, tolerances, and faults. Detailed models often require unacceptable computation times, not only in the PV system design phase but also for implementing operation and maintenance functions and model predictive control algorithms.

These last applications require efficient algorithms for simulating the PV array in any operating condition. For instance, these algorithms need to be compatible with the periodic update of the PV array model during its lifetime, which can assume different values from cell (CL) to CL, especially after many hours of field operation. In addition, nonuniform operating conditions due to partial shadowing, dust, snow, thermal inhomogeneities and possible damages, such as cracks, must be simulated accurately to detect the risk of permanent faults of PV MDs [3].

A fast and accurate real-time PV array simulator also allows to implement control strategies aimed at the global maximum power point tracking [4] and at the dynamic reconfiguration of the connection between PV MDs in the plant [5].

More in general, the PV array simulator is the core of any PV system digital twin (DT), implementing monitoring functions, predictive maintenance strategies and control actions [6]. The DT relies upon a reliable and fast algorithm running a model that is regularly updated by taking into account the actual operating conditions of the PV array.

This article proposes a novel approach to simulate a PV array of any size and at any degree of detail [e.g., sub-CL, CL, submodule (SMD), MD] based on isomorphism. The approach basically detects the similarities among homogeneous parts of the array, so that the nonlinear system of equations to be solved has the minimum rank. Thus, the proposed algorithm is a good candidate tool for the fast simulation of

PV arrays in all the aforementioned applications and on a hardware with limited computational capabilities.

The rest of this article is organized as follows. Section II outlines the state of the art in PV array simulation and contextualizes the contribution of this article. After introducing its origins in the area of general-purpose circuit simulation, the isomorphism-based simulation method is presented step by step in Section III. Section IV shows how the method is formulated and tailored to efficiently simulate any PV field starting from its fundamental building block and going up to the entire array. Finally, in Section V indices are given to measure the performance improvements compared to a conventional simulation approach. These indices are thus used to evaluate the results obtained by simulating current versus voltage (I-V) curves of PV fields undergoing dynamic shading or affected by other mismatching effects. Finally, Section VI concludes this article.

II. STATE OF THE ART IN PV ARRAY SIMULATION

An efficient way to simulate the I-V curve of the PV array is to combine the samples of the I-V curves of the SMD [7], [8] or of the CLs [9], [10], [11] through the Kirchhoff voltage and current laws. Unfortunately, this approach cannot be parameterized, so the adoption of model-based techniques is more frequent.

Some simulation techniques, e.g., the one presented in [12], rely on the physical knowledge of the PV array behavior in mismatched conditions and dynamically adapts the most appropriate PV model—switching among the SDM, a linear model, or a constant voltage model—based on the specific operating conditions of the CLs within the MD. This model adopts an advanced analytical approach named model by zone and achieves a substantial improvement in computation time, significantly reducing it compared to methods available in recent literature. This approach has a limited accuracy when the specific mismatched pattern drives many CLs to work close to their own MPP, thus fully in their nonlinear region. Similarly, the approach presented in [13] exploits an efficient and robust simulation technique, based on wave digital principles, that is tailored to the modular topology of solar arrays. Unfortunately, the results presented in this article give few details and do not allow the reader to appreciate the computational improvement by the approach and to compare its performance with other methodologies.

As it is clear from the literature, the PV array simulation model can operate at different levels of granularity. The more accurate and useful one is at the CL level, since the more critical failures (e.g., hot spots, cracks, ribbon disconnection, and partial shading) can affect any CL in the array. The PV array models available in the literature are based on nonlinear equations, which describe the I-V relation for each CL and often correspond to an equivalent circuit. A circuit simulator solves the electrical network obtained by connecting the CLs to each other to form the entire PV field [14], [15]. Commercial PV MDs include some series-connected SMDs, each of them being made of N_s CLs connected in series and a bypass diode in antiparallel to all of them. The majority of the proposed models assumes that these N_s CLs are equal, thus having exactly the same characteristics, and operate at the same irradiance and temperature. Each PV CL is modeled by a nonlinear I-V equation, which may or may not take internal losses into account. In the first case, the expression might include one or even more exponential terms related to the Shockley effect, and the corresponding equivalent circuit might comprise one or more diodes [16].

The same equations and equivalent circuits can be used at different granularity levels: for instance, it can be assumed that the CLs of each SMD are exactly equal (i.e., same model parameters) and operate in the same conditions (i.e., same irradiance and temperature), so that only one nonlinear I-V equation is needed to describe the whole SMD [17], [18], [19]. Similarly, the model can be scaled up to the whole STR [20], so that a large PV field can be simulated by a system consisting of few nonlinear equations. Such intuitive grouping of equal SMD or STRs was proposed many years ago [21], but often it does not reproduce real conditions accurately, as the mismatches among CLs or SMDs may be so intense that they cannot be grouped in the first place.

A few techniques presented in the recent literature propose innovative approaches to model PV arrays considering the SMD as the smallest granularity level. In contrast, simulating PV arrays at a high granularity level (e.g., down to each CL) leads to accurate results but at the expense of a huge increase in the number of equations to include in the system, with a significant impact on computation time and memory requirements [22], [23]. Moreover, the high rank of the system of equations limits the adoption of too detailed models in real-time and DT-based applications. Particularly, the approaches proposed in [22] and [23] assume that modeling and operating parameters of each CL are different from those ones of the other CLs. Consequently, the system of nonlinear equations to represent an array has a very high rank for large arrays. The system is solved by traditional techniques, with the number of nonlinear equations remaining unchanged regardless of whether the operating conditions are uniform or not [23]. Therefore, the computational burden, memory requirements, and solution time increase significantly with the array size, thus limiting its on-field application by embedded processors. This approach is the basic one that is also considered in this article as a reference. In [22], a simulation technique aimed at improving the solution of the system of nonlinear equations is proposed. It is based on the idea of generating the Jacobian matrix and its inverse by means of a symbolic mathematical procedure, so that the solution of the system of nonlinear equations is sped up. The CL model used in this article is the one published in [24], so that the computation effort and the memory requirements cannot be compared with those ones of techniques adopting different CLs models. Also the approach presented in [22] keeps the array model rank unchanged regardless of the occurrence of uniform or mismatched conditions.

Some strategies for a smart aggregation of similarly operating PV CLs to generate the array I-V curve with a lower computational burden and memory usage have been presented in the recent literature. In [9], the proposed approach acts by grouping the homogeneous CLs of each SMD. This reduces each SMD to a small number of equivalent CLs connected in series, each one representing some homogeneous CLs in the same SMD. The I-V curve of each equivalent CL is computed by using the Bishop's model [24], while the Kirchhoff laws and the nonlinear equation of the bypass diode allow the SMD's I-V curve computation. This procedure is applied to all the SMDs in the array, so that the array I-V curve is obtained by combining the SMDs curves through the Kirchhoff laws according to the array's topology.

In [10], the presence of mismatching conditions is detected through a top-down approach, (i.e., from the array to the CLs). Under homogeneous conditions, the array, STR, or SMD I-V curve is derived by scaling up the CL I-V curve. In case of mismatching, the SMD' I-V curves are firstly determined by using the I-V curves of the CLs they include, then they are combined to compute the whole PV array's curve. Each CL or array element operating uniformly is modeled by neglecting the shunt resistance and accounting for a linear behavior at negative voltages. These assumptions allow the use of nonlinear explicit equations in the array model.

In [11], the array CLs operating in the same conditions are grouped and one I-V per group curve is computed. The same approach is applied to the SMDs and the STRs to derive one I-V curve for each group. Homogeneous SMDs are grouped together, by reducing the computational burden. An optimization algorithm is used to detect and quantify partial shading conditions on the PV STRs and to identify the homogeneous subsections of the array. The proposed approach suffers from some drawbacks: it requires storing in memory the models of the groups of CLs or SMDs operating under the same conditions, as well as all the I-V curves of each SMD or CL. The whole I-V curves must also be computed in cases where only one operating point of the array I-V curve is needed.

This article proposes a novel isomorphic approach to aggregate the homogeneous CLs, SMDs, and STRs. A key feature of the approach is that it can operate at any desired level of granularity of the PV array model by detecting the similarities among homogeneous parts of the PV array and suitably aggregating them. The resulting system of nonlinear equations has a smaller rank than that obtained if each part was modeled by its own nonlinear equation. As it is shown in the following sections, the approach allows the determination of the whole array I-V curve as well as the array current for any assigned voltage value, with a low computational burden and memory usage. These features make the isomorphic-based approach useful for diagnostic purposes and for the real-time simulation needed by a DT.

Section III introduces the isomorphism-based simulation method by referring to the more general area of (electronic) circuit simulation, from which this method originates. Afterward, the method is formulated and tailored to efficiently simulate any PV field by starting from its subcircuit (SC) building block, and going up and up to the entire field. The aggregation is ruled by tags, "implementing" different levels of accuracy in the derived I-V curve. It is shown that these tags, for example, driven by irradiance, can be "loss-less" or "lossy." In the former case, accuracy is preserved. On the contrary, in the latter case, some inaccuracy is accepted to further speed up simulations if, for example, irradiance levels are made discrete and grouped with a given tolerance.

III. ISOMOPHISM-BASED CIRCUITS SIMULATION

Academia and industry proposed several general-purpose circuit simulators. In the field of electronics, the simulation program with integrated circuit emphasis (SPICE and its successors [25]) is one of the most adopted and behaved as a driver for implementing similar tools. The SPICE simulation engine was originally designed by introducing some restrictions to achieve high simulation accuracy. This original paradigm, however, eventually clashed with the increasing integration level and downscaling of electronic devices in integrated circuits (ICs).

A paradigm shift in the SPICE simulation approach was necessary to analyze and design relatively recent and more complex ICs. This trend has led to the emergence of a novel family of accelerated transistor-level simulators (i.e., FAST-SPICE simulators [26], [27]), which resort to innovative heuristics, unique methodologies, and computational techniques. These approaches implement different tradeoffs between simulation speed and accuracy to attain a significant gain in simulation efficiency and capacity. For instance, some methods—hereafter referred to as isomorphism-based techniques—were originally adopted to efficiently simulate memory circuits (i.e., RAMs) by exploiting the presence of CLs with identical topology and a limited number of operating states (e.g., CLs in "read/write" or "idle" mode). This simulation paradigm was recently exploited to simulate modular multilevel converters (MMCs). These converters, which have become the preferred choice in high-voltage direct current systems, are composed of hundreds of SMDs. This multitude of elements poses significant computational challenges to transient simulations [28], [29]. However, just like RAMs, computation times can be profitably reduced through isomorphism-based simulation by exploiting the presence of (almost) identical SMDs in a limited number of operating conditions.

The key feature of isomorphism-based methods is that they group SCs with similar behavior into classes. Instead of simulating each SC individually (as in the case of circuit flattening[1]), these approaches handle only one SC per class. Hence, the number of variables and equations necessary to

[1]A conventional SPICE simulator flattens circuits in the sense that, during netlist reading, the hierarchy among SCs is not preserved. So, all the devices inherent to each SC are included in the netlist and simulated concurrently. This approach does not allow exploiting the peculiarity of the overall circuit's structure and may inevitably result in some wasted effort.

solve the circuit reduces significantly by avoiding the simulation of similar SCs. Despite this, the dynamic evolution of each one of those over time is still retained. Indeed, for each class, the dynamic evolution of one SC is replicated to those of the same group.

To efficiently simulate intrinsically modular circuits, isomorphism-based methods rely on static and dynamic circuit partitioning. Static partitioning, which is carried out at the beginning of the simulation, identifies SCs characterized by the same topology (i.e., the way internal components are connected) and components nature (i.e., constitutive equations). Then, at run time, the dynamic partitioning groups all the static isomorphic SCs with common dynamics in a single equivalent entity. The electrical variables, monitored during circuit operation to establish whether or not some SCs can be merged into a single equivalent entity, are the input electrical quantities, the load conditions, and the state variables (e.g., capacitor voltages and inductor currents). Through dynamic partitioning, instead of simulating each SCs individually, only separate, equivalent entities are considered. It is worth mentioning that static partitioning can be driven in principle also by parameter mismatches in SCs that, otherwise, could be considered identical. At the same time, dynamic partitioning can take into account the spatial and time evolution of the ambient conditions.

To clarify this conceptual description of isomorphism-based methods, let us focus our attention on the generic circuit shown in Fig. 1(a). One can notice the $\mathscr{C}$ component characterized by four SCs connected at the (α_i, β_i) terminal pairs for $i = 1, .., 4$. These SCs are regarded as *identical* in the static isomorphism phase since they share the same topology and their circuit parameter values are the same. No information is provided for the internal structure of $\mathscr{C}$. It is thus possible to identify a class of SCs that, in principle, behaves in the same way. Actually, this is dynamically guaranteed only if, at a given time instant, the voltage across the C capacitor (i.e., the SC state variable) and the v port-voltage are (almost) the same for all of these SCs. In this example, it is not the case as it can be realized by observing the subscripts used to specify these voltages in the circuit schematic. Indeed, there are two classes of dynamically isomorphic entities. To simulate them one can solve, for instance, only the upper SCs and replace the lower ones with two current-controlled current-sources [see Fig. 1(b)]. So doing, instead of flattening the overall circuit solving for the twelve elements connected at the $\mathscr{C}$ ports, it is possible to solve just for the six upper components replicating the i_1 and i_2 currents at the lower ports.

The toy example described previously was added just to convey the operating principle of the isomorphism-based approach. Of course, applying this approach in such a small system grants little to no benefit in terms of simulation efficiency. On the contrary, the benefit becomes tremendously evident when the method is applied to systems where the number of SCs within the classes is high and when the number of classes is minimum. As already mentioned, this is the case

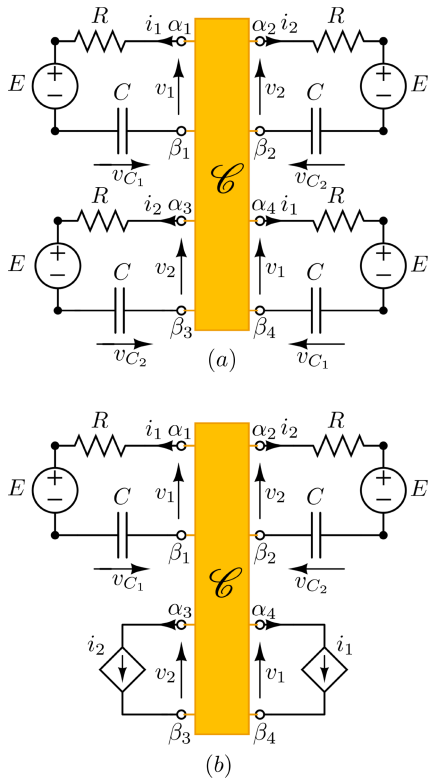

FIGURE 1. Toy example to introduce the basic idea of the isomorphism-based simulation paradigm. In panel (a) one can notice the $\mathscr{C}$ component characterized by four SCs connected at the (α_i, β_i) terminal pairs for $i = 1, \ldots, 4$. These SCs are *statically isomorphic* since their topologies and circuit parameter values are the same. In panel (b) the isomorphic SCs that are *dynamically isomorphic* (viz. that are operating in the same way) are replaced by two proper current-controlled current-sources, thus avoiding circuit flattening.

of RAMs and MMCs, characterized by the connection of a multitude of identical SCs.

This stimulates the curiosity of exploiting isomorphism-based methods in other technological fields wherein this feature frequently occurs in many application cases, such as in PV generators, which consist of the repetition of the same element. The PV CL is the elementary PV device and the PV MD is a "complete and environmentally protected assembly of electrically interconnected PV CLs" [IEC16]. In turn, series-connected PV MDs make up a PV STR, and more STRs constitute the entire PV array. Finally, one or more PV fields, dc cables, and power conditioners make up the whole PV generator, viz. the entire system that uses the PV effect to convert sunlight into electricity [IEC16]. Due to their repetitive structure analogous to that of RAMs and MMCs, PV generators potentially lend themselves to isomorphism-based simulation. To do so, the simulation paradigm grounding on static partitioning in FAST-SPICE simulators could be exploited. Furthermore, in PV generators, partial shading and other mismatched conditions affecting groups of PV CLs frequently happen. By regarding identical PV CLs in different

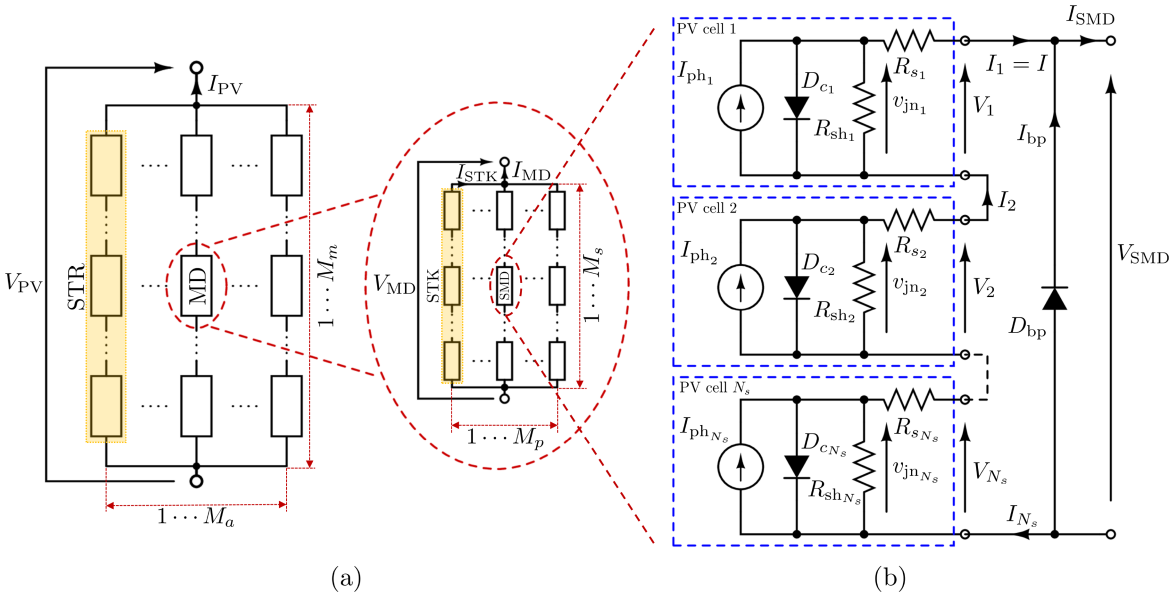

FIGURE 2. **(a) Structure of the generic PV array considered in this work. It is made up of the parallel connection of M_a STRs, each containing M_m MDs connected in series. Each MD is obtained by connecting in parallel M_p STKs of M_s series-connected SMDs. (b) Schematic of an SMD circuit model where N_s CLs are connected in series.**

operating conditions as static SCs in a limited number of operating states, dynamic partitioning could be exploited, too.

IV. ISOMORPHISM-BASED PV ARRAY SIMULATION

The structure of the generic PV array that we consider in this work is shown in Fig. 2(a). For the sake of simplicity, we are assuming that *all* the M_a STRs are made up of M_m MDs connected in series. In the same way, *all* the MDs are assumed to be the parallel connection of M_p stacks (STKs) of M_s series-connected SMD. It is worth noticing that in typical MD architectures $M_p = 1$. The compatibility with cases in which $M_p > 1$ allows to handle half-cut MDs as it will be shown in Section V-B, as well as other more generic and possibly advanced structures that may be developed in the near future.

A. SOLAR CL AND SMD MODEL

Fig. 2(b) shows the schematic of the circuit implementing the model of an SMD resulting from the series connection of N_s CLs possibly connected in parallel to the $D_{\rm bp}$ bypass diode. Each CL is enclosed in a dashed box. Assuming that the CLs are identical, i.e., they share the same operating conditions (e.g., solar irradiance S and CL temperature T_c), and their circuit model parameters are the same (e.g., $R_{s_l} \equiv R_s$ for $l = 1, \ldots, N_s$), it is possible to write[2]

$$I_{\rm ph} - \frac{\overbrace{\frac{V_{\rm SMD}}{N_s} + R_s I}^{v_{{\rm jn}_l}\ (l=1,\ldots,N_s)}}{R_{sh}} - I_s\left(e^{\frac{\frac{V_{\rm SMD}}{N_s}+R_s I}{mV_{\rm th}}} - 1\right) - I = 0 \qquad (1)$$

and[3]

$$I = I_{\rm SMD} - I_{\rm bp}(-V_{\rm SMD}) = I_{\rm SMD} - I_{\rm bps}\left(e^{-\frac{qV_{\rm SMD}}{k_B T_a}} - 1\right). \qquad (2)$$

Typically, $I_{\rm ph} = I_{\rm ph}(S, T_c)$ and $I_s = I_s(T_c)$, and these dependencies can be expressed as

$$I_{\rm ph}(S, T_c) = \frac{S}{S_0}\left(I_{\rm sc0} + \alpha_{I_{sc}}(T_c - T_0)\right),$$

and

$$I_s(T_c) = I_{\rm s0}\left(\frac{T_c}{T_0}\right)^{\frac{3}{m}} e^{\frac{q}{mk_B}\left(\frac{E_{\rm G}(T_0)}{T_0} - \frac{E_{\rm G}(T_c)}{T_c}\right)}$$

where $E_{\rm G}(\chi) = E_{g0\rm K} - \frac{\rho_A \chi^2}{\chi + \rho_B}$ and, for crystalline silicon devices, $E_{g0\rm K} = 1.1557\,\text{eV}$, $\rho_A = 7.021 \cdot 10^{-4}\,\text{eVK}^{-1}$, and $\rho_B = 1108\,\text{K}$ [30]. T_c can be estimated from the T_a ambient temperature, the NOCT and S as shown in (3), where $Z_c = 273.15$, to obtain T_c in K since T_a and NOCT are in °C

$$T_c(T_a, S) = T_a + \frac{\text{NOCT} - 20}{800} S + Z_c. \qquad (3)$$

It is worth noticing that, if we assume to know the value of $V_{\rm SMD}$, we can (numerically) derive $I_{\rm SMD}$ by solving a single nonlinear algebraic equation $\mathscr{E}(V_{\rm SMD}, I_{\rm SMD}) = 0$ that is obtained by replacing (2) in (1). This is not possible if the N_s CLs are not identical. In fact, in that case, some of the $v_{\rm jn}$ junction voltages must be considered among the unknowns, thus enlarging the size of the nonlinear set of equations to

[2]Equation (1) reduces to the implicit equation modeling a single CL if $N_s = 1$ and $V_{\rm SMD} = V_1$.

[3]The driving-point characteristic of the $D_{\rm bp}$ bypass diode is assumed to be computed at $T_{\rm bp} = T_a$. This assumption can be easily removed by making the model more complicated.

be solved. A possible workaround to overcome this issue can be found as follows. Assume that, for instance, the N_s CLs connected in series can be clustered into two groups of N_{s_x} and N_{s_y} CLs, respectively, with $N_{s_x} + N_{s_y} = N_s$. For the sake of simplicity, we can imagine that the circuit model parameters of all the CLs are still identical, but they are operating at two different solar irradiance conditions, say S_x and S_y, and, according to (3), at different temperatures. Since the CLs are connected in series, all the N_{s_x} CLs of the first group are characterized by v_{jn_x}, and those of the second group by v_{jn_y}, with $N_{s_x} v_{\mathrm{jn}_x} + N_{s_y} v_{\mathrm{jn}_y} = V_{\mathrm{SMD}}$. By exploiting the Lambert $\mathscr{W}(\cdot)$ function [31] it is possible to rewrite (1) as

$$V_{\mathrm{SMD}} = \sum_{k\in\{x,y\}} N_{s_k} \left(R_{sh}(I_{\mathrm{ph}_k} + I_{s_k}) - (R_{sh} + R_s)I - mV_{\mathrm{th}_k}\mathscr{W}(\theta_{V_k})\right) \tag{4}$$

where

$$\theta_{V_k} = \frac{R_{sh}I_s}{mV_{\mathrm{th}_k}} e^{\frac{R_{sh}(I_{\mathrm{ph}}+I_s-I)}{mV_{\mathrm{th}_k}}}.$$

Now, if we assume once more to know the value of V_{SMD}, we can derive I_{SMD} by solving a single nonlinear algebraic equation $\widetilde{\mathscr{E}}(V_{\mathrm{SMD}}, I_{\mathrm{SMD}}) = 0$. This equation is obtained by replacing (2) in (4), instead of enlarging the size of the nonlinear set of equations to be solved by including v_{jn_x} and v_{jn_y} among the unknowns.

B. ISOMORPHISM TAGS

In order to identify isomorphic elements in a given PV array it is necessary to introduce an operative criterion based on quantitative indicators. At first, we choose a $\mathscr{V}$ dimensional real vector associated with every basic building block of a PV array. Whether the former is the SMD or the CL, that vector is referred to as either Ξ^{SMD} or Ξ^{CL}, respectively. This vector can be viewed as a *tag* used to decide if two entities are homogeneous, viz. *isomorphic*, and contains the value of $\mathscr{V}$ quantities that are chosen *a priori* as *isomorphism variables*. These variables can be parameters of the CL model (e.g., R_s, R_{sh}, m, etc.) or variables defining the CL or the SMD operating condition (e.g., S and T_c). In case the SMD is selected as the basic building block of a PV array, the parameters of all the CLs within a SMD are assumed to be identical. In general, it is even possible to have a Ξ^{CL} tag containing some parameters of the SMD the CL belongs to, for instance related to the D_{bp} bypass diode.

To introduce through an example how these tags can be propagated from the basic building blocks of a PV array up to STRs, passing through STKs and MDs, let us consider the four MDs in Fig. 3 labeled from (a) to (d) where, for the sake of simplicity, we chose $M_p = 1$ and $M_s = 5$. Assuming that the basic building block is the SMD, we suppose the SMDs in Fig. 3 to be characterized by three different tags, say Ξ_x^{SMD}, Ξ_y^{SMD}, and Ξ_z^{SMD}, for the black, white, and gray blocks, respectively. These tags may be associated, for instance, with different irradiance values.

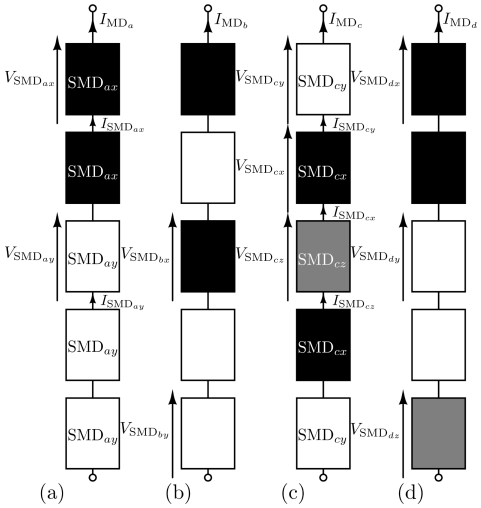

FIGURE 3. Four MDs are represented made up of a single STK ($M_p = 1$) of five series connected SMDs ($M_s = 5$). In all the cases, the voltage across each MD is assumed to be the same (V_{MD}). The SMDs exhibit three different tags, say Ξ_x^{SMD}, Ξ_y^{SMD}, and Ξ_z^{SMD}, for the black, white, and gray blocks, respectively. When using isomorphism-based techniques, the (a) and (b) cases [as well as the (c) and (d) ones] are analogous because they include the same number of elements for each class (i.e., SMDs of same color): the order in which these elements are connected is irrelevant.

The example shows how different SMDs can be clustered in isomorphic groups. In fact, if we assume that all the MDs share the same voltage V_{MD}, it is easy to be convinced that $V_{\mathrm{SMD}_{ax}} = V_{\mathrm{SMD}_{bx}}$, $V_{\mathrm{SMD}_{ay}} = V_{\mathrm{SMD}_{by}}$, $V_{\mathrm{SMD}_{cx}} = V_{\mathrm{SMD}_{dx}}$, $V_{\mathrm{SMD}_{cy}} = V_{\mathrm{SMD}_{dy}}$, and $V_{\mathrm{SMD}_{cz}} = V_{\mathrm{SMD}_{dz}}$. Furthermore, $I_{\mathrm{MD}_a} = I_{\mathrm{MD}_b}$ and $I_{\mathrm{MD}_c} = I_{\mathrm{MD}_d}$. It is thus possible to identify two prototypes of isomorphic MDs, say MD_a and MD_c, made up of subsets of isomorphic SMDs. In particular, MD_a involves two classes of SMDs, say SMD_{ax} (with the Ξ_x^{SMD} tag) and SMD_{ay} (with the Ξ_y^{SMD} tag), each one including $M_{s_{ax}} = 2$ and $M_{s_{ay}} = 3$ elements, respectively. MD_a is representative of the (a) and (b) cases. The MD_c prototype [representative for the (c) and (d) cases] brings in three classes of SMDs, say SMD_{cx}, SMD_{cy}, and SMD_{cz}, each one including $M_{s_{cx}} = M_{s_{cy}} = 2$ or $M_{s_{cz}} = 1$ elements, respectively. It is worth noting that, when using isomorphism-based techniques, the (a) and (b) cases [as well as the (c) and (d) ones] are analogous because they include the same number of elements for each class (i.e., SMDs of same color): the order in which these elements are connected is *irrelevant*.

In terms of isomorphism tags, it is possible to conceive the Ξ^{MD} new tag defined at MD level. By defining the $||$ symbol as the concatenation operator,[4] the MD_a prototype is identified by $\Xi_a^{\mathrm{MD}} = 2||\Xi_x^{\mathrm{SMD}}||3||\Xi_y^{\mathrm{SMD}}$, whereas $\Xi_c^{\mathrm{MD}} = 2||\Xi_x^{\mathrm{SMD}}||2||\Xi_y^{\mathrm{SMD}}||1||\Xi_z^{\mathrm{SMD}}$.

[4]It is worth noticing that, even if at the basic building block level tags are vectors of real numbers, the concatenation operator make them simple labels. So doing, for instance, $2||\Xi_x^{\mathrm{SMD}}$ does not correspond to multiply by 2 the elements of the Ξ_x^{SMD} vector, but to juxtapose 2 and Ξ_x^{SMD}.

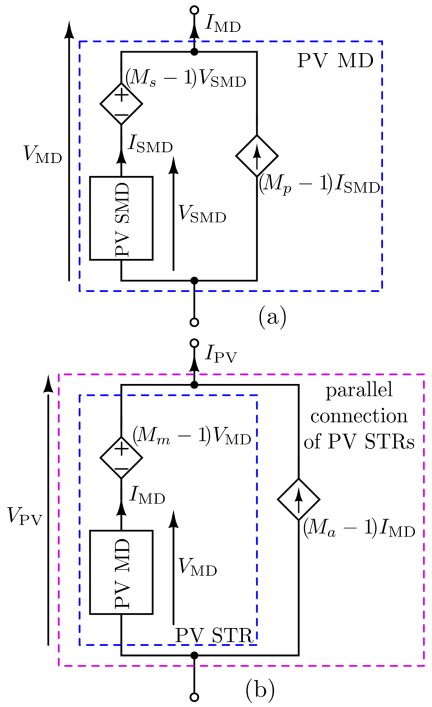

FIGURE 4. (a) Equivalent model of a MD made up of identical SMDs sharing the same operating conditions. (b) Equivalent model of the parallel connection of M_a STRs each one made up of the series connection of M_m MDs represented in panel (a).

The same way of reasoning can be used to derive the STK tag (Ξ^{STK}) starting from the tags of the isomorphic series-connected SMDs. The MD tags, when $M_p > 1$, is based on the tags of the isomorphic parallel-connected STKs within.

Finally at STR level, the Ξ^{STR} tag is obtained from the tags of the isomorphic MDs connected in series within the STR. For instance, let us assume to have an STR with $M_m = 10$ MDs connected in series, three of them of type MD_a, and seven of type MD_c. Then, we can define $\Xi^{\text{STR}} = 3||\Xi_a^{\text{MD}}||7||\Xi_c^{\text{MD}}$ that, in turn, can be expanded by exploiting the expression of Ξ_a^{MD} and Ξ_c^{MD} introduced previously. So doing, the tag at the highest level of description is expressed as a function of the tag of the basic building blocks of the PV array.

Definition 4.1 (Lossless isomorphism): Two entities of type $\xi \in \{\text{CL, SMD, STK, MD, STR}\}$ are lossless isomorphic (or simply isomorphic) if they share the same Ξ^{ξ} isomorphism tag.

C. PV ARRAY SOLUTION WITH ALL ISOMORPHIC PV SMDS

Let us now assume that the basic building block of a PV array is the SMD. The easiest scenario to introduce isomorphism-based simulation is when all the SMDs are isomorphic, viz. they share the same Ξ^{SMD} tag.

In this case, each MD (viz. PV panel) can be represented by the equivalent SC shown in Fig. 4(a). It corresponds to the parallel connection of M_p STKs of M_s SMDs connected in series. The equivalent circuit in Fig. 4(a) can be derived by having in mind that isomorphic SMDs connected in series exhibit the same V_{SMD} voltage, which can be mimicked by exploiting a linear voltage-controlled voltage-source, and $V_{\text{MD}} = M_s V_{\text{SMD}}$. In the same way, $I_{\text{MD}} = M_p I_{\text{SMD}}$ and this can be achieved by a current-controlled current-source mimicking I_{SMD}. As shown in Fig. 4(b), an analogous representation can be used to describe the parallel connection of M_a STRs, where the latter results from the series connection of M_m MDs.

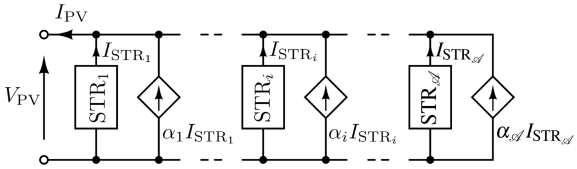

FIGURE 5. Equivalent model of a PV array containing $\mathscr{A}$ clusters of STRs, each one made up of M_{a_i} homogeneous entities ($\alpha_i = M_{a_i} - 1$). Since the STRs are connected in parallel, $V_{\text{STR}_i} = V_{\text{PV}}$ for $i = 1, \ldots, \mathscr{A}$.

The I_{PV} current in Fig. 4(b) can be derived as a function of V_{PV} by numerically solving the nonlinear equation $\mathscr{E}(V_{\text{SMD}}, I_{\text{SMD}}) = 0$ with $V_{\text{SMD}} = \frac{V_{\text{PV}}}{(M_m M_s)}$. The solution provides I_{SMD} and, finally, $I_{\text{PV}} = I_{\text{SMD}} M_p M_a$.[5] Overall, the behavior of the entire solar array can be determined by solving a *single nonlinear scalar* equation.

D. PV ARRAY SOLUTION WITH HETEROGENEOUS PV SMDS

In this section we introduce a family of more complex scenarios, in which the basic building block of a PV array is once more the SMD, but SMDs may not share the same Ξ^{SMD}. At first, a bottom-up approach is used to derive the isomorphism tag of every element composing the PV array. These tags will be used to achieve the equivalent reduced order circuit model of the PV array.

In particular, the M_a STRs connected in parallel forming a PV array can be organized in $\mathscr{A}$ clusters of M_{a_i} homogeneous elements, with $M_a = \sum_{i=1}^{\mathscr{A}} M_{a_i}$. Each one of these clusters is represented by a prototype of STRs, say STR_i, with the Ξ_i^{STR} tag. The PV array can be represented by the equivalent model in Fig. 5. The ith STR represented in Fig. 5 contains, in principle, $\mathscr{M}_i$ clusters of MDs, each one made up of $M_{m_{ij}}$ homogeneous elements, with $M_m = \sum_{j=1}^{\mathscr{M}_i} M_{m_{ij}}$ and can be represented by the equivalent STR in Fig. 6. The jth of these $\mathscr{M}_i$ clusters is identified by an MD prototype, say MD_{ij} (with the Ξ_{ij}^{MD} tag) that in turn is made up of M_p parallel-connected STKs of SMDs connected in series. These STKs can be organized in $\mathscr{P}_{ij}$ clusters each one made up of $M_{p_{ijk}}$ homogeneous elements, being $M_p = \sum_{k=1}^{\mathscr{P}_{ij}} M_{p_{ijk}}$. The MD_{ij} can be represented through the equivalent circuit in Fig. 7.

[5] A DC/DC converter typically regulates the voltage of the PV array V_{PV} to achieve maximum power transfer through the MPPT and allowing the PV array connection to a DC bus. In the light of the above, V_{PV} can be regarded as a controlled variable.

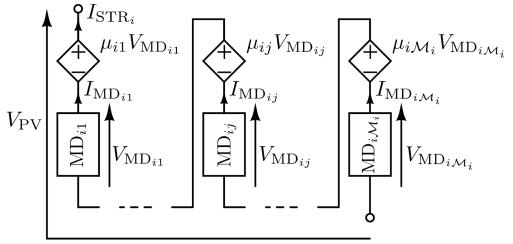

FIGURE 6. Equivalent model of an STR, say STR_i, containing $\mathscr{M}_i$ clusters of MDs, each one made up of $M_{m_{ij}}$ homogeneous entities ($\mu_{ij} = M_{m_{ij}} - 1$). Since the MDs are connected in series, $I_{\mathrm{MD}_{ij}} = I_{\mathrm{STR}_i}$ for $j = 1, \ldots, \mathscr{M}_i$.

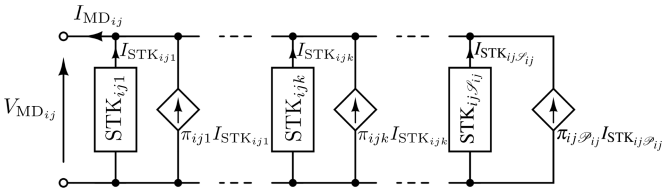

FIGURE 7. Equivalent model of an MD, say MD_{ij}, containing $\mathscr{P}_{ij}$ clusters of STKs, each one made up of $M_{P_{ijk}}$ homogeneous entities ($\pi_{ijk} = M_{P_{ijk}} - 1$). Since the STKs are connected in parallel, $V_{\mathrm{STK}_{ijk}} = V_{\mathrm{MD}_{ij}}$ for $k = 1, \ldots, \mathscr{P}_{ij}$.

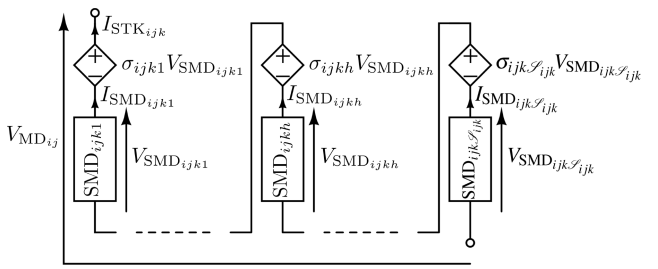

FIGURE 8. Equivalent model of an stack (STK), say STK_{ijk}, containing $\mathscr{S}_{ijk}$ clusters of SMDs, each one made up of $M_{s_{ijkh}}$ homogeneous entities ($\sigma_{ijkh} = M_{s_{ijkh}} - 1$). Since the SMDs are connected in series, $I_{\mathrm{SMD}_{ijkh}} = I_{\mathrm{STK}_{ijk}}$ for $h = 1, \ldots, \mathscr{S}_{ijk}$.

The kth of these $\mathscr{P}_{ij}$ clusters is identified by a representative STK, say STK_{ijk} (with the $\Xi^{\mathrm{STK}_{ijk}}$ tag), which is in turn made up of $\mathscr{S}_{ijk}$ clusters of SMDs. The hth of them contains $M_{s_{ijkh}}$ homogeneous elements, say SMD_{ijkh} (with the $\Xi^{\mathrm{SMD}}_{ijkh}$ tag and being $M_s = \sum_{h=1}^{\mathscr{S}_{ijk}} M_{s_{ijkh}}$) and it admits the equivalent circuit reported in Fig. 8. It is worth mentioning that the overall PV array clustered architecture described previously reduces to the one reported in Fig. 4 if all the SMDs are homogeneous. In this case, $\mathscr{A} = \mathscr{M}_{\mathscr{A}} = \mathscr{P}_{\mathscr{A}\mathscr{M}} = \mathscr{S}_{\mathscr{A}\mathscr{M}\mathscr{P}} = 1$.

The topological equations governing the PV array can be written as

$$\sum_{i=1}^{\mathscr{A}} M_{a_i} I_{\mathrm{STR}_i} - I_{\mathrm{PV}} = 0 \tag{5a}$$

$$\sum_{j=1}^{\mathscr{M}_i} M_{m_{ij}} V_{\mathrm{MD}_{ij}} - V_{\mathrm{PV}} = 0 \quad \left(i = 1, \ldots, \mathscr{A}\right) \tag{5b}$$

$$\sum_{k=1}^{\mathscr{P}_{ij}} M_{p_{ijk}} I_{\mathrm{STK}_{ijk}} - I_{\mathrm{STR}_i} = 0 \quad \begin{pmatrix} i = 1, \ldots, \mathscr{A} \\ j = 1, \ldots, \mathscr{M}_i \end{pmatrix} \tag{5c}$$

$$\sum_{h=1}^{\mathscr{S}_{ijk}} M_{s_{ijkh}} V_{\mathrm{SMD}_{ijkh}} - V_{\mathrm{MD}_{ij}} = 0 \quad \begin{pmatrix} i = 1, \ldots, \mathscr{A} \\ j = 1, \ldots, \mathscr{M}_i \\ k = 1, \ldots, \mathscr{P}_{ij} \end{pmatrix} \tag{5d}$$

$$I_{\mathrm{SMD}_{ijkh}} - I_{\mathrm{STK}_{ijk}} = 0 \quad \begin{pmatrix} i = 1, \ldots, \mathscr{A} \\ j = 1, \ldots, \mathscr{M}_i \\ k = 1, \ldots, \mathscr{P}_{ij} \\ h = 1, \ldots, \mathscr{S}_{ijk} \end{pmatrix} \tag{5e}$$

and are completed by the nonlinear equations linking the current and voltage of each representative SMD (i.e., $\mathscr{E}_{ijkh}(V_{\mathrm{SMD}_{ijkh}}, I_{\mathrm{SMD}_{ijkh}}) = 0$). On the whole, the PV array is fully described by a set of $\mathscr{Z}_{\mathrm{SMD}}$ equations with $\mathscr{Z}_{\mathrm{SMD}}$ unknowns, where

$$\mathscr{Z}_{\mathrm{SMD}} = \underbrace{1}_{(5a)} + \underbrace{\mathscr{A}}_{(5b)} + \sum_{i=1}^{\mathscr{A}} \left(\underbrace{\mathscr{M}_i}_{(5c)} + \sum_{j=1}^{\mathscr{M}_i} \left(\underbrace{\mathscr{P}_{ij}}_{(5d)} + \underbrace{2 \sum_{k=1}^{\mathscr{P}_{ij}} \mathscr{S}_{ijk}}_{(5e),\, \mathscr{E}_{\mathrm{ijkh}}} \right) \right). \tag{6}$$

E. PV ARRAY SOLUTION WITH HETEROGENEOUS PV CLS

The more complex scenario shows up when the basic building block of the PV array becomes the single CL. In this case, isomorphism among STRs within the PV array, MDs within an STR, STKs within an MD, and SMDs within a STK does not stop at SMD level. The granularity of the model increases since SMDs may be heterogeneous because, for instance, the solar irradiance S is different between the CLs of the SMD itself.

If we focus on SMD_{ijkh} (i.e., the representative of the hth cluster of isomorphic SMDs), within the kth cluster of isomorphic STKs, within the jth cluster of isomorphic MDs, within the i-th cluster of isomorphic STRs (see Section IV-D), we may assume that its series connected CLs can be in turn grouped in $\mathscr{C}_{ijkh}$ clusters of isomorphic elements, being $\sum_{q=1}^{\mathscr{C}_{ijkh}} N_{s_{ijkhq}} = N_s$. To take into account these new sets of isomorphic entities, (5) must be enlarged with new equations and new unknowns[6]

$$\begin{aligned} &\textstyle\sum_{q=1}^{\mathscr{C}_{ijkh}} N_{s_{ijkhq}} \left(v_{\mathrm{jn}_{ijkhq}} - R_s I_{ijkh} \right) - V_{\mathrm{SMD}_{ijkh}} = 0 \\ &I_{ijkh} + I_{\mathrm{bp}_{ijkh}} - I_{\mathrm{SMD}_{ijkh}} = 0 \quad \begin{pmatrix} i = 1, \ldots, \mathscr{A} \\ j = 1, \ldots, \mathscr{M}_i \\ k = 1, \ldots, \mathscr{P}_{ij} \\ h = 1, \ldots, \mathscr{S}_{ijk} \end{pmatrix} \end{aligned} \tag{7a}$$

$$I_{ijkh} - I_{ijkhq} = 0 \quad \begin{pmatrix} i = 1, \ldots, \mathscr{A} \\ j = 1, \ldots, \mathscr{M}_i \\ k = 1, \ldots, \mathscr{P}_{ij} \\ h = 1, \ldots, \mathscr{S}_{ijk} \\ q = 1, \ldots, \mathscr{C}_{ijkh} \end{pmatrix}. \tag{7b}$$

[6]Here, for the sake of simplicity, we assume that all the CLs share the same R_s.

Furthermore, the nonlinear equations involved by SMD_{ijkh} do not depend anymore on $V_{\text{SMD}_{ijkh}}$ and $I_{\text{SMD}_{ijkh}}$ but each cluster of isomorphic CLs introduces the constraint $\mathscr{E}_{ijkhq}(v_{\text{jn}_{ijkhq}}, I_{ijkhq}) = 0$. The total number of equations governing the PV array becomes

$$\mathscr{Z}_{\text{CL}} = \underbrace{1}_{(5a)} + \underbrace{\mathscr{A}}_{(5b)} + \sum_{i=1}^{\mathscr{A}} \left(\underbrace{\mathscr{M}_i}_{(5c)} + \sum_{j=1}^{\mathscr{M}_i} \left(\underbrace{\mathscr{P}_{ij}}_{(5d)} + \sum_{k=1}^{\mathscr{P}_{ij}} \left(\underbrace{3\mathscr{S}_{ijk}}_{(5e),(7a)} + \underbrace{2 \sum_{h=1}^{\mathscr{S}_{ijk}} \mathscr{C}_{ijkh}}_{(7b),\, \mathscr{E}_{ijkhq}} \right) \right) \right)$$

with $\mathscr{Z}_{\text{CL}} \gg \mathscr{Z}_{\text{SMD}}$.

F. LOSSLESS AND LOSSY ISOMORPHISM MODELING

The procedure, as described, is lossless because the elementary building blocks of the PV array are considered isomorphic according to Definition IV.1 if they have *the same tag*. This definition can be weakened if lossy isomorphism is admissible at building block level.

Definition 4.2 (Lossy isomorphism): Two entities of type $\xi \in \{\text{CL}, \text{SMD}\}$, with isomorphic tag given by Ξ_1^ξ and Ξ_2^ξ, respectively, are lossy isomorphic if $|\Xi_1^\xi - \Xi_2^\xi| < \epsilon \in \mathbb{R}^{\mathscr{V}}$. In this case a unique $\widehat{\Xi}^\xi$ tag is introduced to represent both.

It is worth recalling that in this definition $\Xi_{1,2}^\xi \in \mathbb{R}^{\mathscr{V}}$ and the inequality must be satisfied componentwise. Once lossy isomorphism is applied at building block level, thus identifying tags that represents cluster of similar but not identical entities, those tags are propagated at higher levels up to STRs. The overall isomorphism-based PV array model, grounding on a tradeoff between accuracy and computational burden, becomes an approximate model. It worth pointing out that, unfortunately, it is not possible to systematically predict the sensitivity of the simulation accuracy w.r.t. to different values of the ϵ threshold introduced in Definition IV.2. This is basically due to the fact that, in general, the effect of this parameter, whose choice reflects on how isomorphism tags are clustered despite being different, depends, for instance, on which parameters are used to define the tags themselves. The shape of the $P_{\text{PV}}(V_{\text{PV}})$ curve can be highly influenced by the adoption of the lossy clustering approach, as it will be exemplified in the case study reported in Section V-A. This depends also on the exponential nonlinearity of the PV CL equations, which is extremely sensitive w.r.t. variations in their parameters.

G. SPEEDING UP THE SIMULATION

It is important to underline that, even if the isomorphic paradigm is not chosen, whenever a general-purpose circuit-simulation approach is not adopted, the simulation of a generic PV array can be accelerated.

For instance, as we anticipated in Section IV-A, it is possible to keep unchanged the number of unknowns/equations describing the array from the SMD-level to the CL-level. This can be done by exploiting the Lambert $\mathscr{W}(\cdot)$ function for each SMD_{ijkh}. It was exemplified in (4) by assuming that the N_s series connected CL of the SMD are clustered into two groups. This can be easily generalized for each SMD_{ijkh} characterized by $\mathscr{C}_{ijkh}$ clusters of CLs. Such an approach comes at the price of introducing some unavoidable approximations in computing $\mathscr{W}(\cdot)$ [31]. Nevertheless, it is worth paying this price since, keeping unchanged the numbers of unknowns, this approach allows to easily extend the proposed isomorphism-based simulation method, which was developed by assuming the SMD as the basic building block of the overall PV array, to the case where the single CL becomes the elementary unit. In other words, by exploiting the Lambert function, even in the second case it is possible to solve $\mathscr{Z}_{\text{SMD}}$ equations instead of $\mathscr{Z}_{\text{CL}}$.

A further speed up can be achieved by exploiting the series connection of SMDs within a single STK and of CLs within a single SMD. It allows dropping some of the variables introduced in (5) and (7). In particular, one can avoid defining the $I_{\text{SMD}_{ijkh}}$ currents in (5e) and the I_{ijkhq} currents in (7b). Overall it is possible to reduce $\mathscr{Z}_{\text{SMD}}$ to

$$\mathscr{Z}_{\text{SMD}}^{\text{red}_1} = \underbrace{1}_{(5a)} + \underbrace{\mathscr{A}}_{(5b)} + \sum_{i=1}^{\mathscr{A}} \left(\underbrace{\mathscr{M}_i}_{(5c)} + \sum_{j=1}^{\mathscr{M}_i} \left(\underbrace{\mathscr{P}_{ij}}_{(5d)} + \underbrace{\sum_{k=1}^{\mathscr{P}_{ij}} \mathscr{S}_{ijk}}_{\mathscr{E}_{ijkh}} \right) \right)$$

and $\mathscr{Z}_{\text{CL}}$ to

$$\mathscr{Z}_{\text{CL}}^{\text{red}_1} = \underbrace{1}_{(5a)} + \underbrace{\mathscr{A}}_{(5b)} + \sum_{i=1}^{\mathscr{A}} \left(\underbrace{\mathscr{M}_i}_{(5c)} + \sum_{j=1}^{\mathscr{M}_i} \left(\underbrace{\mathscr{P}_{ij}}_{(5d)} + \sum_{k=1}^{\mathscr{P}_{ij}} \left(\underbrace{2\mathscr{S}_{ijk}}_{(7a)} + \underbrace{\sum_{h=1}^{\mathscr{S}_{ijk}} \mathscr{C}_{ijkh}}_{\mathscr{E}_{ijkh}} \right) \right) \right).$$

A useful consideration can be done when $M_p = 1$, i.e., each MD is made up of a single STK of series connected SMDs, and, consequently $\mathscr{P}_{ij} = 1$ $(\forall\, i, j)$. In this case, all the SMDs in a given STR, although belonging to different MDs, are connected in series. The PV array can be solved as if it were composed of $M_m M_s$ MDs with only one SMD in each of them. The equations in (5) can be reduced avoiding the introduction of the I_{STK} and I_{SMD} currents (only I_{STR} are necessary), and of the V_{SMD} voltages (only V_{MD} are necessary). So doing, (5) reduces to

$$\sum_{i=1}^{\mathscr{A}} M_{a_i} I_{\text{STR}_i} - I_{\text{PV}} = 0 \tag{8a}$$

$$\sum_{j=1}^{\mathscr{M}_i} M_{m_{ij}} V_{\text{MD}_{ij}} - V_{\text{PV}} = 0 \qquad \left(i = 1, \ldots, \mathscr{A}\right) \tag{8b}$$

completed by the nonlinear equations linking the current and the voltage of each representative SMD, i.e, $\mathscr{E}_{ij}(V_{\text{MD}_{ij}}, I_{\text{STR}_i}) = 0$. On the whole

$$\mathscr{Z}_{\text{SMD}}^{\text{red}_2} = \underbrace{1}_{(8a)} + \underbrace{\mathscr{A}}_{(8b)} + \sum_{i=1}^{\mathscr{A}} \underbrace{\mathscr{M}_i}_{\mathscr{E}_{ij}}.$$

TABLE 1. Parameters of the PV CL for the Traditional MD

R_s	5 mΩ	R_{sh}	4 kΩ	I_{sc0}	5 A
I_{s0}	11.6 nA	I_{bps}	1 pA	m	1.2
$\alpha_{I_{sc}}$	3.25 mAK^{-1}	T_a	25 °C	NOCT	45 °C

Analogously, (7) reduces to

$$\begin{matrix} \sum_{q=1}^{\mathscr{C}_{ij11}} N_{s_{ij11q}} \left(v_{\mathrm{jn}_{ij11q}} - R_s I_{ij11} \right) \\ -V_{\mathrm{MD}_{ij}} = 0 \\ I_{ij11} + I_{\mathrm{bp}_{ij11}} - I_{\mathrm{STR}_i} = 0 \end{matrix} \qquad \begin{pmatrix} i = 1, \ldots, \mathscr{A} \\ j = 1, \ldots, \mathscr{M}_i \end{pmatrix} \tag{9a}$$

completed by $\mathscr{E}_{ij11q}(v_{\mathrm{jn}_{ij11q}}, I_{ij11}) = 0$, and

$$\mathscr{Z}_{CLs}^{\mathrm{red}_2} = \underbrace{1}_{(8a)} + \underbrace{\mathscr{A}}_{(8b)} + \sum_{i=1}^{\mathscr{A}} \left(\underbrace{2\mathscr{M}_i}_{(9a)} + \sum_{j=1}^{\mathscr{M}_i} \underbrace{\mathscr{C}_{ij11}}_{\mathscr{E}_{ij11q}} \right).$$

V. SIMULATION RESULTS

The PV array simulator based on isomorphism was implemented in MATLAB [32] on an 11th Gen IntelCore™ i9-11900H @2.50GHz, eight cores, 16 virtual processors, 64 GB RAM memory Microsoft Windows 11 Pro Version 10.0 computer. The simulator was implemented as a single-thread program.[7]

A. MONOCRYSTALLINE PV ARRAY

The PV array is made up of $M_m = 10$ series connected MDs organized in $M_a = 1$ STRs. Each MD contains a single STK (i.e., $M_p = 1$) with $M_s = 3$ SMDs of $N_s = 20$ CLs each. The schematic of each SMD is shown in Fig. 2(b) and the parameter values of the CL are reported in Table 1. The MDs are arranged in a single row of ten elements; the overall PV array can be represented by a matrix of 20 × 30 CLs.

The PV array was simulated under 37 different shading conditions corresponding to a shaded area diagonally moving from the bottom-left corner to the up-right corner of the PV array. In the first and last frames the PV array is not shaded ($S = S_0$) and completely shaded ($S = 0\mathrm{Wm}^{-2}$), respectively. In the intermediate frames, the S solar irradiance assumes different values at different CLs of the PV array. In the left column of Fig. 9, frames number 5, 10, 15, 20, and 25 are reported from top to bottom. The variable used for the isomorphism tags was the S solar irradiance.

For each frame, we computed the $I_{\mathrm{PV}}(V_{\mathrm{PV}})$ driving point characteristic of the PV array by varying V_{PV} from 0 V to 0.6 V$N_sM_sM_m = 360$ V with a discrete step equal to 0.5 V. The PV array was solved 721 times per frame.

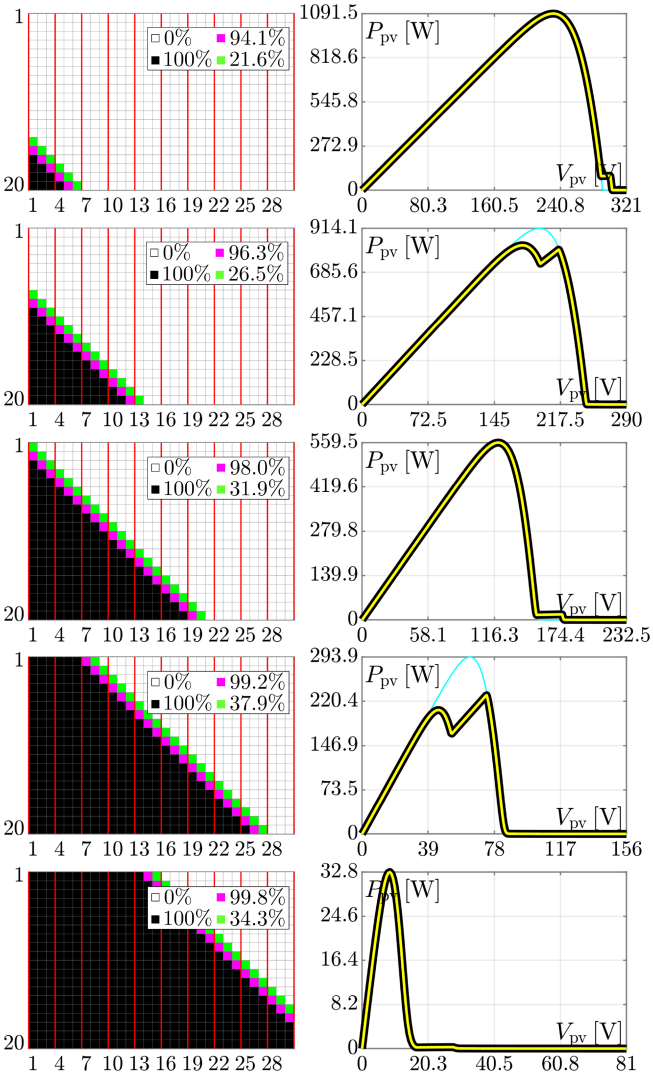

FIGURE 9. From top to bottom each pair of panels refers to frame number 5, 10, 15, 20, and 25 of the 37 different shadowing conditions that were simulated. In the left-column, the shadowing percentage of the CLs is reported in the legend of each panel. The right column reports the electrical power supplied by the PV array: black, yellow, and cyan colored curves were obtained by exploiting the PAN SPICE-like circuit simulator, the lossless isomorphism based simulation approach at CL level through the Lambert function $\mathscr{W}(\cdot)$, and its lossy counterpart ($\epsilon = 0.5$), respectively.

Lossless isomorphism was applied by considering the CL as the basic building block. The array is represented using the formalism introduced in the previous sections and the Lambert $\mathscr{W}(\cdot)$ function is used to solve each SMD_{ijkh}. The $\mathscr{Z}_{\mathrm{CL}} = \mathscr{Z}_{\mathrm{SMD}}$ number of equations to be solved runs then from 6 (the array is made up of fully isomorphic MDs) to 82 (the array is made up of fully nonisomorphic MDs). If the $v_{\mathrm{jn}_{ijkhq}}$ and i_{ijkhq} variables were introduced, the $\mathscr{Z}_{\mathrm{CL}}$ number of equations to be solved would jump from 9 to 1312.

Since each MD contains only a single STK of SMDs, it is also possible to model the PV array as the series connection of $M_mM_s = 30$ SMDs. Using the approaches reported in Section IV-G, the minimum and maximum number of equations that must be solved are 3 (the array is made up of fully

[7] As far as multithreading is concerned, the first and simplest modification is to solve in parallel the $\mathscr{A}$ PV STRs representing all the possible clusters of these high-level elements sharing the same V_{PV} driving voltage. Other possible programming solutions are less trivial and for example can act on the parallel execution of the Newton method and on the evaluations of the models of PV elements. In these cases the overhead introduced in handling threads, which can possibly run for a very short CPU time, must be carefully considered.

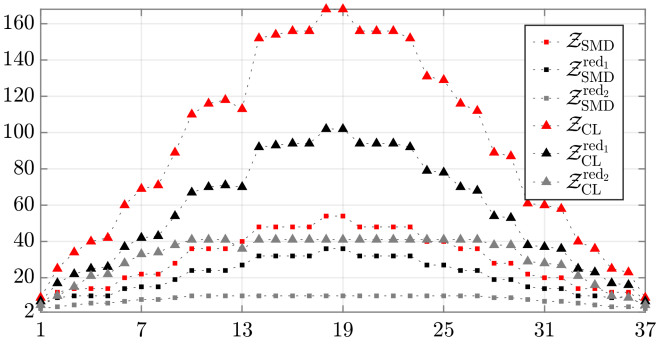

FIGURE 10. Number of equations to be solved for any PV array model and for any frame obtained for each position of the shadow: the horizontal axis refers to the shadow frame number and the vertical axis to the corresponding number of modeling equations for each PV array model, from the one referring to the PV MD granularity level (gray squares) to the most detailed one (red triangles), which describes the array CL by CL.

isomorphic SMDs and the Lambert $\mathcal{W}(\cdot)$ function is used to solve SMD_{1111}) and 662 (the array is made up of fully nonisomorphic SMDs and the Lambert $\mathcal{W}(\cdot)$ function is not used to solve SMD_{ij11}). The number of equations to be solved per frame, according to the adopted different strategies, is reported in Fig. 10. This figure reveals the very significant effect of the proposed isomorphism-based approach in reducing the number of equations describing the mismatched PV array. In the worst case of the shadowing pattern corresponding to the #18 and #19 conditions, the number of nonlinear equations in the system to be solved is reduced by the 75%, being scaled down from 662 equations to 168 equations.

In all the 37 simulations performed for the case study, the isomorphism procedure for clustering elements took less than 5 ms. The CPU time needed to perform clustering is a small fraction of the total simulation time, since only simple basic numerical operations are performed on the elements in the data-structure used to identify isomorphic elements. These operations are manly sorting, reordering and comparisons; complex floating point operations such as multiplications and divisions are not performed. Total CPU time needed for clustering can largely vary [see Fig. 13(c)], depending on the size of the problem at hand and on the number of variables used as clustering indicators, but it remains a tiny fraction of the total simulation time, due to its implementation "simplicity." The minimum solution time measured for the array made up of fully isomorphic SMDs was 0.08 s, when the $\mathcal{W}(\cdot)$ Lambert function was used and simulations were sped up by solving $\mathcal{Z}_{\mathrm{SMD}}^{\mathrm{red}_2} = 3$ equations. The maximum solution time (1.32 s) was measured for $\mathcal{Z}_{\mathrm{SMD}} = 48$, while for the maximum value of $\mathcal{Z}_{\mathrm{SMD}} = 54$ the solution time was 1.17s. Since the circuit is highly nonlinear and the Newton method is used to solve its equations, it cannot be taken for granted that the maximum simulation time corresponds to the maximum number of equations to be solved.

The right-hand side panels of Fig. 9 show the electrical power supplied by the PV array. The yellow trace corresponds to the results obtained through the lossless isomorphism-based approach, while the black one has been derived by simulating the PV array using a SPICE-like circuit simulator,[8] where *circuit flattening* is employed. In this specific case, the total number of equations to solve turned out to be 1321[9] and the circuit consisted of 1891 devices. It can be seen that the results obtained by simulating the PV array at CL level through the lossless isomorphism-based approach (which relies on the Lambert function $\mathcal{W}(\cdot)$) perfectly adhere to those obtained by exploiting the SPICE-like circuit simulator. As a consequence, we did not implement in MATLAB the complete solution method, which is not based on $\mathcal{W}(\cdot)$. The choice of using a well-known and largely used simulator at industrial level such as a SPICE-like simulator was a thoughtful decision. We believe that it allows for a direct comparison of basically any simulation tool tailored to PV arrays, and thus the indirect fair derivation of relative performances. Furthermore SPICE-like simulators, such as for example LTspice, are freely distributed.

We also applied the lossy isomorphism approach to simulate the 37 frames. Making reference to Definition IV.2, we chose $\epsilon = 0.5$ (quite large relative threshold). It corresponds to assume that each CL can be either completely shadowed or not shadowed at all (in the left-hand side panels of Fig. 9 the magenta and green CLs become black and white, respectively). So doing, the number of equations to be solved can be further reduced, but this comes at the price of losing accuracy in the simulation of the I-V curve, as shown by the cyan traces in the right-hand side panels of Fig. 9.

B. HALF-CUT PV ARRAY

This second case study has two goals: it explains how to handle half-cut MDs and it shows how the proposed isomorphism-based simulation approach can be effectively used to address parameter mismatches in PV CLs beyond just those affected by partial shading. To prove these features, we pick as an example of PV mismatch that induced by the PV CLs cracking phenomenon in half-cut MDs.

Over the years, there has been a decrease in the thickness of the PV CLs in order to reduce production costs. However, PV CLs have become more fragile and vulnerable to thermal and mechanical stresses. Consequently, this can lead to the formation of cracks during the production and transportation of the PV model, as well as after its installation. Cracking can reach both sides of the CL and, in certain cases, can cause the disconnection of parts of the CL from its electrical circuit so that they become partially inactive, causing a reduction in the current produced by the CL itself. Here, the effect of cracking is modeled by using the experimental results reported in [36] where up to five cracks were produced in c-Si CLs by applying

[8] The PAN circuit simulator was adopted [33], [34], [35].

[9] It is worth noting that the number of equations is slightly different from $\mathcal{Z}_{\mathrm{CL}} = 1312$, which was previously mentioned for the case of fully nonisomorphic MDs (i.e., the worst case possible). This is due to the fact that PAN is a general-purpose simulator: as such, it may introduce additional equations to compute the solution of the PV array.

TABLE 2. Parameters of the CL for the Half-Cut MD

R_s	4.818 mΩ	R_{sh}	9.023 Ω	I_{sc0}	5.440 A
I_{s0}	11.39 pA	I_{bps}	1 pA	m	1.081
$\alpha_{I_{sc}}$	4.352 mAK^{-1}	T_a	25 °C	NOCT	44 °C

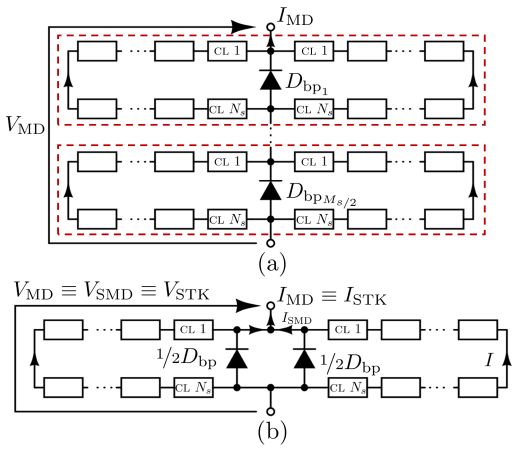

FIGURE 11. (a) Schematic of a generic half-cut PV MD made up of the series connection of $\frac{M_s}{2}$ pairs of two SMDs connected in parallel and sharing the same bypass diode. Each SMD contains N_s series connected PV CLs. (b) According to Fig. 2(a), an half-cut MD can be viewed as $\frac{M_s}{2}$ equivalent classical MDs connected in series. Each of them contains, the parallel connection of two STKs each one including one SMD. Since in Fig. 2(b) every SMD in a given STK has its own bypass diode, whereas in the half-cut technology a bypass diode is shared by two parallel connected SMDs, we divide by two the I_{bps} current of the bypass diode in each SMD.

a uniaxial mechanical tension around the y-axis on the upper glass layer of the CL.

The considered PV array is made up of $M_a = 3$ STRs of $M_m = 17$ series connected half-cut MDs each. Each MD contains $M_s = 6$ SMDs (connected in pairs) of $N_s = 22$ CLs each. The nominal parameter values of the equivalent single diode model of the PV CL are reported in Table 2. On the whole, the array includes 3366 CLs. The generic architecture of an half-cut MD is shown in Fig. 11(a). According to the generic layout adopted in this article and reported in Fig. 2(a) and Section IV-G, it is convenient to model each STR of the PV array as a series connection of 17×3 MDs, each one containing $M_p = 2$ STKs including a unique SMD with $N_s = 22$ CLs [see Fig. 11(b)].

We performed 100 simulations of the PV fields by randomly choosing 3% of the CLs affected by one crack, 1% by two cracks, and another 1% by three cracks, each of these having an I-V curve, as shown in Fig. 12. The variables used for the isomorphism tags were R_s, R_{sh}, I_{sc0}, I_{s0}, and m. For each trial we computed the $I_{PV}(V_{PV})$ driving point characteristic of the PV array by varying V_{PV} from 0 V to 0.75 V$N_sM_sM_m = 841.5$ V with a discrete step equal to 0.5 V. The PV array model was solved 1684 times per trial.

Since $M_p = 2$, the modeling approach leading to $\mathscr{Z}_{CL}^{red_2}$ and $\mathscr{Z}_{SMD}^{red_2}$ cannot be used. The PV array can then be simulated at the CL-level in four different ways only. By assuming that the PV CLs are either all heterogeneous (the isomorphism approach cannot be adopted) or all homogeneous (maximum speed up of the isomorphism approach), it is possible to derive the maximum and minimum number of equations to be solved, as reported in Table 3.

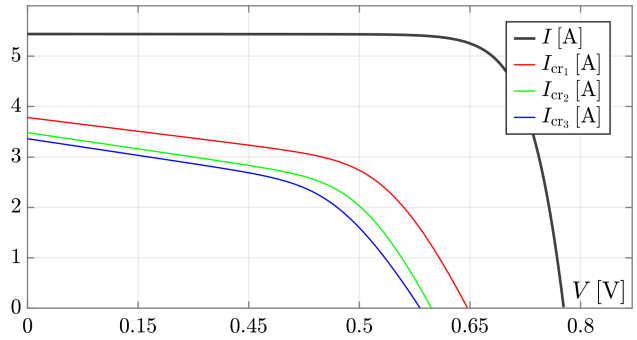

FIGURE 12. Black colored curve corresponds to the $I - V$ driving point characteristic of the PV CL for the parameter values reported in Table 2. In case of 1, 2, or 3 cracks, the $I - V$ driving point characteristic reduces to the red, green, and blue colored curves, respectively. The corresponding parameter values of the single diode model of the damaged CL are: $R_s \in \{21.80, 21.55, 28.80\}$ mΩ, $R_{sh} \in \{0.5969, 0.4957, 0.4810\}$ Ω, $I_{sc0} \in \{3.897, 3.610, 3.536\}$ A, $I_{s0} \in \{0.9092, 1.636, 1.819\}$ μA, and $m \in \{1.597, 1.536, 1.508\}$.

TABLE 3. Maximum and Minimum Number of Equations to Be Solved

	All heterogeneous	All homogeneous
$\mathscr{Z}_{CL}$	14845	9
$\mathscr{Z}_{CL}^{red_1}$	3676	5
$\mathscr{Z}_{SMD}$	1075	6
$\mathscr{Z}_{SMD}^{red_1}$	769	5

The PV array was simulated also using the SPICE-like circuit simulator adopted for the case study reported in Section V-A. In each one of the 100 random configurations, for any value of the V_{PV} input voltage, the total number of equations to solve turned out to be 14 534 and the circuit consisted of 21 115 devices.[10] It is worth mentioning that, in the worst case of Table 3, the isomorphism-based simulator must solve almost the same number of equations of the SPICE-like circuit simulator, but $\mathscr{Z}_{SMD}^{red_1}$ yields a drop of 95% in the worst case, reaching 99.9% in the best case.

Ultimately, the PV array was simulated at the CL-level by using the two most convenient approaches (i.e., the ones that resort to the $\mathscr{W}(\cdot)$ Lambert function). The violin plots[11] reported in Fig. 13(a) summarize the performance of the isomorphism simulation method in term of the huge percentage drop of equations to be solved w.r.t. the SPICE-like circuit simulator.

In Fig. 13(b) the t_{SOL}^{iso} computation time needed to solve the PV array by adopting the strategy corresponding to $\mathscr{Z}_{SMD}^{red_1}$ is

[10]Note that the number of equations is slightly different from 14 845, that is, the highest value reported in Table 3. Once again, as also stated in footnote[9], this is due to how PAN simulator simulator computes the solution of the PV array.

[11]A violin plot is a combination of a box plot and a kernel density plot. Specifically, it starts with a box plot and then adds a rotated kernel density plot to each side of the box plot.

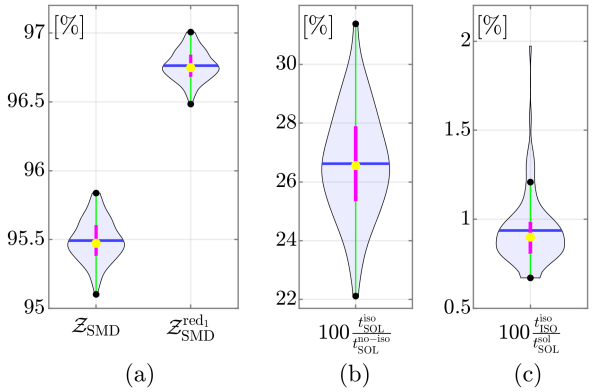

FIGURE 13. **(a) Violin plot of the percentage drop of the number of equations to be solved to simulate the PV array at the CL level using the Lambert $\mathscr{W}(\cdot)$ function, in the $\mathscr{Z}_{\text{SMD}}$ and $\mathscr{Z}^{\text{red}_1}_{\text{SMD}}$ cases, w.r.t. the SPICE-like circuit simulator. (b) Violin plot of the percentage ratio between the $t^{\text{iso}}_{\text{SOL}}$ computation time (in the $\mathscr{Z}^{\text{red}_1}_{\text{SMD}}$ case) and $t^{\text{no-iso}}_{\text{SOL}}$, i.e., the computation time needed to solve the PV array when the isomorphism procedure is not exploited but the $\mathscr{W}(\cdot)$ Lambert function only is used to solve the PV SMD. (c) Violin plot of the relative computation time needed to perform clustering with respect to the entire simulation time. The yellow solid circle markers in the violin plots correspond to the median value and the horizontal blue bar is the mean indicator. The magenta bars represent the IQR, viz. the spread difference between the 75th and 25th percentiles of the data. The black solid circle markers, connected by a green bar, represent the upper adjacent value (i.e., the largest observation that is less than or equal to the third quartile plus 1.5 × IQR) and the lower adjacent value (i.e., the smallest observation that is greater than or equal to the first quartile minus 1.5 × IQR).**

compared to the $t^{\text{no-iso}}_{\text{SOL}}$ computation time needed when the isomorphism procedure is not exploited but the $\mathscr{W}(\cdot)$ Lambert function only is used to solve the PV SMD [according to (4) in the case of $N_s = 22$ heterogeneous CLs in each SMD]. In this case, even if the equations to be solved are always equal to 769, the computation time varies in the 100 configurations because the system is nonlinear and an iterative numerical solution method is used. In Fig. 13(c) the computation time needed to apply the isomorphism procedure is reported.

VI. CONCLUDING REMARKS

In this article, a novel approach to the simulation of PV arrays is introduced. The isomorphism-based approach recognizes similarities among the operating conditions and single diode model parameters of the PV array subsections and minimizes the rank of the system of nonlinear equations that models the array. It is worth mentioning that it is not possible to provide an analysis of how the method performs as the PV array size increases since, in fact, its performance does not basically depend on the array size. To be more precise, the isomorphism clustering process becomes more time-consuming for larger arrays but this is not the bottleneck of the proposed simulation approach. The computational burden is due to the solution of the (nonlinear) system of equations that govern the electrical behavior of the circuit. The time required to solve these equations depends on the heterogeneousness of the PV building blocks, viz. to which extent the isomorphism principle applies to the considered array in a specific working condition. In Section IV, some formulas where derived that allow to compute the number of equations to be solved as a function of the number of isomorphic classes that one can identify at different level (from CLs to STRs). Of course, in the unlucky case in which there are no isomorphic classes of elements in the PV array, the isomorphism-based simulation approach coincides with a traditional solution method that scales with the dimension of the PV array as the solution complexity of any circuit scales with the number of its components and nodes. Under these circumstances, lossy isomorphism may be used to boost simulation speed at the expense of a decrease in accuracy (which ultimately depends on the ε tolerance).

The two realistic examples proposed refer to a an array that is progressively affected by a slow time-varying partial shading and to an array of half-cut CLs, some of them affected by cracks. In both cases, the isomorphism-based approach leads to a huge reduction in the rank of the array model, dropping it down to 75% and 95%, respectively. Consequently, the computation time significantly drops by more than 20%. This performance makes the proposed approach a good candidate for a DT application. Indeed, further work is in progress to implement the approach in a low cost embedded platform and integrating it into the control, monitoring, and diagnostic system of a real PV plant.

REFERENCES

[1] IEA, "Renewables 2023 - Analysis and forecast to 2028," International Energy Agency, Tech. Rep., 2023.
[2] IEA-PVPS, "Snapshot of global PV markets - 2024," International Energy Agency, Tech. Rep. IEA-PVPS T1-42, 2024.
[3] Z. U. Khan et al., "A review of degradation and reliability analysis of a solar PV module," IEEE Access, vol. 12, pp. 185036–185056, 2024.
[4] S. M. A. Bakar, Z. Dongya, R. A. Ur, O. Khmaies, and H. Hamam, "An adapted model predictive control MPPT for validation of optimum GMPP tracking under partial shading conditions," *Sci. Rep.*, vol. 14, no. 1, pp. 1–30, 2024.
[5] X. Fang and Q. Yang, "Dynamic reconfiguration of photovoltaic array for minimizing mismatch loss," *Renewable Sustain. Energy Rev.*, vol. 191, 2024, Art. no. 114160. [Online]. Available: https://www.sciencedirect.com/science/article/pii/S1364032123010183
[6] PhotoVoltaic - European Technology & Innovation Platform, "Research challenges in PV reliability," Tech. Rep., 2020.
[7] M. Kermadi, V. J. Chin, S. Mekhilef, and Z. Salam, "A fast and accurate generalized analytical approach for PV arrays modeling under partial shading conditions," *Sol. Energy*, vol. 208, pp. 753–765, Sep. 2020.
[8] C. R. Sánchez Reinoso, D. H. Milone, and R. H. Buitrago, "Simulation of photovoltaic centrals with dynamic shading," *Appl. Energy*, vol. 103, pp. 278–289, Mar. 2013.
[9] E. Díaz-Dorado, J. Cidrás, and C. Carrillo, "Discrete I–V model for partially shaded PV-arrays," *Sol. Energy*, vol. 103, pp. 96–107, May 2014.
[10] A. Bennani-Ben Abdelghani and H. Ben Attia Sethom, "Modeling PV installations under partial shading conditions," *SN Appl. Sci.*, vol. 2, no. 4, pp. 1–9, Apr. 2020.
[11] Y. Li, K. Ding, J. Zhang, F. Chen, X. Chen, and J. Wu, "A fault diagnosis method for photovoltaic arrays based on fault parameters identification," *Renewable Energy*, vol. 143, pp. 52–63, Dec. 2019.
[12] A. Carabali-Isajar, M. Orozco-Gutierrez, E. Franco-Mejía, G. Spagnuolo, and J. Restrepo, "FPGA-based real-time simulation of mismatched photovoltaic arrays," *Heliyon*, vol. 8, no. 7, 2022, Art. no. e09969.
[13] A. Bernardini, A. Sarti, P. Maffezzoni, and L. Daniel, "Wave digital-based variability analysis of electrical mismatch in photovoltaic arrays," in *Proc. 2018 IEEE Int. Symp. Circuits Syst.*, 2018, pp. 1–5.

[14] K. Abdulmawjood, S. Alsadi, S. S. Refaat, and W. G. Morsi, "Characteristic study of solar photovoltaic array under different partial shading conditions," *IEEE Access*, vol. 10, pp. 6856–6866, 2022.
[15] P. K. Bonthagorla and S. Mikkili, "Performance analysis of PV array configurations (SP, BL, HC and TT) to enhance maximum power under non-uniform shading conditions," *Eng. Rep.*, vol. 2, no. 8, Aug. 2020, Art. no. e12214.
[16] G. Petrone, C. A. Ramos-Paja, and G. Spagnuolo, *Photovoltaic Sources Modeling*. Chichester, U.K.: Wiley, 2017.
[17] G. Petrone, G. Spagnuolo, and M. Vitelli, "Analytical model of mismatched photovoltaic fields by means of Lambert W-function," *Sol. Energy Mater. Sol. Cells*, vol. 91, no. 18, pp. 1652–1657, Nov. 2007.
[18] M. Orozco-Gutierrez, J. Ramirez-Scarpetta, G. Spagnuolo, and C. Ramos-Paja, "A technique for mismatched PV array simulation," *Renewable Energy*, vol. 55, pp. 417–427, Jul. 2013.
[19] J. D. Bastidas-Rodriguez, J. M. Cruz-Duarte, and R. Correa, "Mismatched series–parallel photovoltaic generator modeling: An implicit current–voltage approach," *IEEE J. Photovolt.*, vol. 9, no. 3, pp. 768–774, May 2019.
[20] J. Bastidas, E. Franco, G. Petrone, C. Ramos-Paja, and G. Spagnuolo, "A model of photovoltaic fields in mismatching conditions featuring an improved calculation speed," *Electric Power Syst. Res.*, vol. 96, pp. 81–90, Mar. 2013.
[21] H. Patel and V. Agarwal, "MATLAB-Based modeling to study the effects of partial shading on PV array characteristics," *IEEE Trans. Energy Convers.*, vol. 23, no. 1, pp. 302–310, Mar. 2008.
[22] M. Orozco-Gutierrez, J. Ramirez-Scarpetta, G. Spagnuolo, and C. Ramos-Paja, "A method for simulating large PV arrays that include reverse biased cells," *Appl. Energy*, vol. 123, pp. 157–167, Jun. 2014.
[23] E. A. Sarquis Filho, C. A. F. Fernandes, and P. J. Da C. Branco, "A complete framework for the simulation of photovoltaic arrays under mismatch conditions," *Sol. Energy*, vol. 213, pp. 13–26, Jan. 2021.
[24] J. W. Bishop, "Computer simulation of the effects of electrical mismatches in photovoltaic cell interconnection circuits," *Sol. Cells*, vol. 25, no. 1, pp. 73–89, 1988.
[25] L. Nagel, "SPICE2: A computer program to simulate semiconductor circuits," EECS Department University of California, Berkeley, CA, USA, Tech. Rep. UCB/ERL M520, 1975.
[26] J. White and A. Sangiovanni-Vincentelli, *Relaxation Techniques for the Simulation of VLSI Circuits*, vol. 20. Norwell, MA, USA: Kluwer, 1987.
[27] B. Chawla, H. Gummel, and P. Kozak, "MOTIS-An MOS timing simulator," *IEEE Trans. Circuits Syst.*, vol. 22, no. 12, pp. 901–910, Dec. 1975.
[28] D. del Giudice, A. M. Brambilla, D. Linaro, and F. Bizzarri, "Isomorphic circuit clustering for fast and accurate electromagnetic transient simulations of MMCs," *IEEE Trans. Energy Convers.*, vol. 37, no. 2, pp. 800–810, Jun. 2022.
[29] D. del Giudice, F. Bizzarri, D. Linaro, and A. M. Brambilla, *Modular Multilevel Converter Modelling and Simulation for HVDC Systems: State of the Art and a Novel Approach*. Berlin, Germany: Springer Nature, 2022.
[30] Y. Varshni, "Temperature dependence of the energy gap in semiconductors," *Physica*, vol. 34, no. 1, pp. 149–154, 1967.
[31] E. I. Batzelis, G. Anagnostou, C. Chakraborty, and B. C. Pal, "Computation of the Lambert W function in photovoltaic modeling," in *ELECTRIMACS 2019*, W. Zamboni and G. Petrone, Eds. Cham, Switzerland: Springer Int. Publishing, 2020, pp. 583–595.
[32] T. M. Inc., "MATLAB version: 24.2.0.2806996 (R2024b)," Natick, MA, USA, 2024. [Online]. Available: https://www.mathworks.com
[33] F. Bizzarri and A. Brambilla, "PAN and MPanSuite: Simulation vehicles towards the analysis and design of heterogeneous mixed electrical systems," in *Proc. 2017 New Generation of CAS*, Genova, Italy, Sep. 2017, pp. 1–4.
[34] F. Bizzarri, A. Brambilla, G. Storti Gajani, and S. Banerjee, "Simulation of real world circuits: Extending conventional analysis methods to circuits described by heterogeneous languages," *IEEE Circuits Syst. Mag.*, vol. 14, no. 4, pp. 51–70, Oct.–Dec. 2014.
[35] D. Linaro, D. del Giudice, F. Bizzarri, and A. Brambilla, "PanSuite: A free simulation environment for the analysis of hybrid electrical power systems," *Electric Power Syst. Res.*, vol. 212, pp. 1–7, 2022.
[36] S. A. Alves dos Santos, J. P. N. Torres, C. A. F. Fernandes, and R. A. Marques Lameirinhas, "The impact of aging of solar cells on the performance of photovoltaic panels," *Energy Convers. Manage.: X*, vol. 10, 2021, Art. no. 100082. [Online]. Available: https://www.sciencedirect.com/science/article/pii/S2590174521000076